nature immunology

IL-7 coordinates proliferation, differentiation and *Tcra* recombination during thymocyte β-selection

Amine Boudil[1,2], Irina R Matei[1], Han-Yu Shih[3], Goce Bogdanoski[1], Julie S Yuan[1], Stephen G Chang[1], Bertrand Montpellier[1,2], Paul E Kowalski[1], Veronique Voisin[4], Shaheena Bashir[4], Gary D Bader[4,5], Michael S Krangel[3] & Cynthia J Guidos[1,2]

Signaling via the pre–T cell antigen receptor (pre-TCR) and the receptor Notch1 induces transient self-renewal (β-selection) of TCRβ$^+$ CD4$^-$CD8$^-$ double-negative stage 3 (DN3) and DN4 progenitor cells that differentiate into CD4$^+$CD8$^+$ double-positive (DP) thymocytes, which then rearrange the locus encoding the TCR α-chain (*Tcra*). Interleukin 7 (IL-7) promotes the survival of TCRβ$^-$ DN thymocytes by inducing expression of the pro-survival molecule Bcl-2, but the functions of IL-7 during β-selection have remained unclear. Here we found that IL-7 signaled TCRβ$^+$ DN3 and DN4 thymocytes to upregulate genes encoding molecules involved in cell growth and repressed the gene encoding the transcriptional repressor Bcl-6. Accordingly, IL-7-deficient DN4 cells lacked trophic receptors and did not proliferate but rearranged *Tcra* prematurely and differentiated rapidly. Deletion of *Bcl6* partially restored the self-renewal of DN4 cells in the absence of IL-7, but overexpression of *BCL2* did not. Thus, IL-7 critically acts cooperatively with signaling via the pre-TCR and Notch1 to coordinate proliferation, differentiation and *Tcra* recombination during β-selection.

During intrathymic T cell development, signaling via the receptor Notch1 maintains cell survival and promotes commitment to the T cell lineage as CD44$^+$CD25$^-$ cells that are at CD4$^-$CD8$^-$ double-negative stage 1 (DN1) differentiate into CD44$^+$CD25$^+$ DN2 cells and CD44^{lo}CD25$^+$ DN3a cells[1]. Mice lacking the gene encoding interleukin 7 (IL-7) or its receptor (IL-7R) have very few DN2 and DN3 cells, in part because these cells depend on IL-7 signaling to induce expression of *Bcl2*, which encodes a pro-survival molecule (Bcl-2)[2]. Indeed, transgenic expression of human *BCL2* (refs. 3,4) or deletion of *Bax* or *Bim*, which encode pro-apoptotic molecules[5,6], substantially restores both the DN2-DN3 and mature CD4$^+$CD8$^-$ or CD4$^-$CD8$^+$ single-positive (SP) compartments in mice deficient in the α-chain of IL-7R (*Il7r*$^{-/-}$) or the common γ-chain (*Il2rg*$^{-/-}$). Thus, IL-7 induces Bcl-2-mediated survival of DN2-DN3a progenitor cells committed to the T cell lineage as they become quiescent and rearrange gene segments in loci encoding the T cell antigen receptor (TCR) γ-chain (*Tcrg*), δ-chain (*Tcrd*) and β-chain (*Tcrb*). The subsequent proliferation and differentiation of progenitors of αβ T cells requires successful *Tcrb* rearrangement and expression of intracellular TCRβ (icTCRβ) protein to form the pre-TCR signaling complex and initiate β-selection. Although IL-7R expression persists through the early stages of β-selection, the importance of IL-7 signaling in this process has not been resolved.

Signaling via the pre-TCR and signaling via Notch1 act together to initiate β-selection[7] by inducing quiescent DN3a cells to downregulate expression of genes encoding components of the RAG recombinase (*Rag1* and *Rag2*) and become large cycling DN3b cells that upregulate genes encoding the transferrin receptor CD71 (*Tfrc*) and other trophic receptors[8]. These changes induced by the pre-TCR and Notch1 promote rapid self-renewal of DN3b cells as they lose expression of the T cell–activation marker and cytokine receptor CD25 (IL-2Rα) and differentiate sequentially into cycling DN4 cells, CD4$^-$CD8$^+$ immature single-positive (ISP) cells and early CD4$^+$CD8$^+$ double-positive (eDP) blast cells, which then cease proliferating and become quiescent late DP (lDP) cells. However, it is unclear whether signaling via the pre-TCR and Notch1 is sufficient to maintain trophic responses, proliferation and differentiation during β-selection *in vivo*.

Expression of *Rag1* and *Rag2* decreases precipitously after the DN3a stage, so efficient rearrangement of *Tcra* requires re-expression of *Rag1* and *Rag2* in DP thymocytes[9]. Recombination of *Tcra* normally initiates in eDP cells through the use of the farthest 3′ gene segments encoding the α-chain variable region (V_α) and furthest 5′ gene segments encoding the α-chain joining region (J_α). If DP thymocytes fail to be positively selected after primary rearrangement of *Tcra*, secondary rearrangements occur that use progressively more distal gene segments encoding V_α (5′ end) and J_α (3′ end), but only in non-cycling lDP cells[10]. The enhancer of *Tcra* (E_α), located 3′ of the array encoding J_α, modifies chromatin at the *Tcra* locus to make the 3′ gene segments encoding V_α and 5′ gene segments encoding J_α accessible to the RAG recombinase, which facilitated the synapsis and recombination of these segments[11]. Although *Tcra* rearrangement is restricted to DP thymocytes, E_α may be activated as early as the DN4 stage by transcription factors induced by signaling via the

[1]Program in Developmental and Stem Cell Biology, Hospital for Sick Children Research Institute, Toronto, Canada. [2]Department of Immunology, University of Toronto, Toronto, Canada. [3]Department of Immunology, Duke University Medical Center, Durham, North Carolina, USA. [4]The Donnelly Centre, University of Toronto, Toronto, Canada. [5]Department of Molecular Genetics, University of Toronto, Toronto, Canada. Correspondence should be addressed to C.J.G. (cynthia.guidos@sickkids.ca).

Received 1 December 2014; accepted 10 February 2015; published online 2 March 2015; doi:10.1038/ni.3122

pre-TCR[12]. During the pro-B cell–to–pre-B cell transition induced by the pre–B cell antigen receptor (pre-BCR), IL-7 induces proliferation and represses rearrangement of the locus encoding the immunoglobulin κ-chain complex by an epigenetic mechanism dependent on the transcription factor STAT5 (refs. 13,14). STAT5 also represses expression of the gene encoding Bcl-6 to prevent apoptosis induced by the tumor suppressor p53 during recombination of the locus encoding the immunoglobulin light chain in pre-B cells[15,16]. Bcl-6 is best known as a transcriptional repressor with critical functions in germinal center responses and as a potent B cell oncoprotein[17]. Notably, thymocytes substantially upregulate *Bcl6* as proliferation ceases during the DN3-DP transition (as reported by the Immunological Genome Project), but the regulation and functions of Bcl-6 during T cell development have not been defined.

There are conflicting reports on the role of IL-7 signaling in β-selection. IL-7R expression is not lost until the ISP stage[18], but DN4 thymocytes have been reported to be unresponsive to IL-7 (ref. 19). Studies using antibodies to block IL-7 signaling *in vitro* have concluded that IL-7 signaling is dispensable for the β-selection of DN3 cells[20]. In contrast, another study has reported, through the use of a similar approach, that IL-7 signaling is required for the survival of DN4 cells but not their proliferation[21]. Other studies in which IL-7 signaling was artificially augmented *in vitro* have concluded that IL-7 signaling actively inhibits β-selection, in part by impairing expression of the transcription factor–encoding genes *Tcf7*, *Lef1* and *Rorc*[18]. Therefore, *in vitro* studies have reached conflicting conclusions on the importance of IL-7 signaling during β-selection.

Here we found that early post-β-selection DN3b and DN4 thymocytes responded to IL-7 *in vitro* and *in vivo*. IL-7 signaling rapidly induced many genes encoding molecules involved in protein translation, cell growth and metabolism and also repressed *Bcl6*. Accordingly, we found that IL-7 was needed *in vivo* for robust clonal expansion, to enforce the canonical DN3b-DN4-ISP-DP differentiation sequence and to prevent premature rearrangement of *Tcra* in DN thymocytes. Thus, we have identified a previously unknown role for IL-7 signaling during β-selection that includes repression of *Bcl6* to allow self-renewal of DN4 cells. In contrast to the functions of IL-7 at earlier and later stages of T cell development, the functions of IL-7 during β-selection could not be recapitulated by Bcl-2.

RESULTS

IL-7 signaling in post-β-selection DN thymocytes

We first compared the expression and function of IL-7R in DN thymocytes before and after β-selection. In contrast to published studies[19], we used icTCRβ to positively identify β-selected cells in the heterogeneous DN3 and DN4 subsets (**Supplementary Fig. 1**). As expected, pre-selection icTCRβ$^-$ DN3a cells were IL-7R^{hi} and robustly phosphorylated STAT5 after stimulation with IL-7 *in vitro* (**Fig. 1a**). Post-selection DN3b and DN4 cells also expressed IL-7R, and stimulation with IL-7 induced phosphorylation of STAT5 (**Fig. 1a**). The amounts of IL-7R and IL-7-induced phosphorylation of STAT5 were highest in DN3b cells and lowest in DN4 cells (**Fig. 1a**). Nonetheless, stimulation with IL-7 increased the survival of DN3a, DN3b and DN4 cells to a similar extent (**Fig. 1a**). Thus, pre-selection DN3a thymocytes and post-selection DN3b-DN4 thymocytes were similarly responsive to IL-7-mediated survival signaling *in vitro*. Notably, fresh *ex vivo* DN3b and DN4 *Il7r*$^{+/+}$ thymocytes had considerably larger amounts of phosphorylated STAT5 and more mouse Bcl-2 than did those from *Il7r*$^{-/-}$ mice (**Fig. 1b**), which indicated that they responded to physiological levels of IL-7 produced intrathymically.

To determine if human Bcl-2 was able restore both the pre-β-selection compartment and post-β-selection compartments in IL-7R-deficient mice, we generated *Il7r*$^{-/-}$ mice with transgenic expression of the gene encoding human Bcl-2 (*BCL2*) under control of the proximal promoter of the gene encoding the tyrosine kinase Lck. This induced expression of human Bcl-2 in some DN2 cells

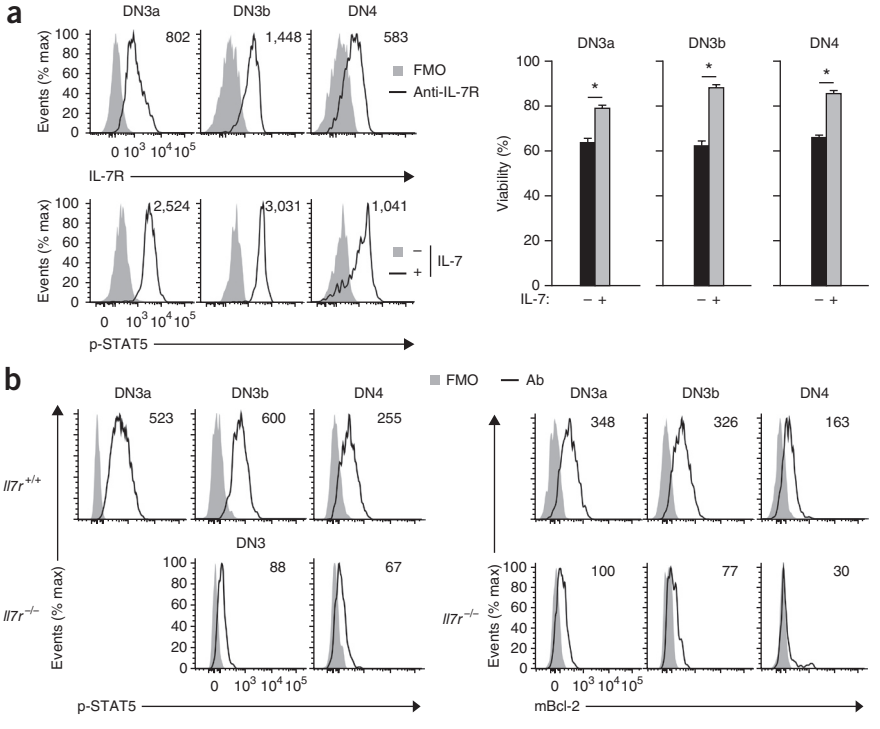

Figure 1 Expression and function of IL-7R in pre- and post-β-selection thymocytes. (**a**) Flow cytometry of DN3a (CD25$^+$icTCRβ$^-$), DN3b (CD25$^+$icTCRβ$^+$) and DN4 (CD25$^-$icTCRβ$^+$) thymocytes from wild-type mice (gating strategy, **Supplementary Fig. 1**), stained with antibody to IL-7R (Anti-IL-7R), plotted with the fluorescence-minus-one background control (FMO) (top left), or cultured for 20 min with (+) or without (–) IL-7 and stained with antibody to phosphorylated STAT5 (p-STAT5) (bottom left); right, viability of cells cultured for 10–24 h with or without IL-7 and then, analyzed by staining with propidium iodide and flow cytometry. *$P \leq 0.0001$ (unpaired two-tailed Student's *t*-test). (**b**) Flow cytometry of DN3a, DN3b and DN4 *Il7r*$^{+/+}$ or *Il7r*$^{-/-}$ thymocytes fixed, permeabilized and stained with antibody to phosphorylated STAT5 (left), or stained with antibody to mouse Bcl-2 (mBcl-2), plotted with background control as in **a** (right). Due to limited cellularity, phosphorylated STAT5 was analyzed in total DN3 cells from *Il7r*$^{-/-}$ mice. Numbers in plots indicate normalized median fluorescence intensity of each marker, calculated by subtraction of the median fluorescence intensity of the fluorescence-minus-one control from that of fully stained cells (**a**, top right, and **b**) or of phosphorylated STAT5, calculated by subtraction of the median fluorescence intensity of cells cultured without IL-7 from that of cells cultured with IL-7 (**a**, bottom left). Data are representative of three independent experiments with similar results (mean and s.d. of two biological replicates with two technical replicates per group in **a**, right).

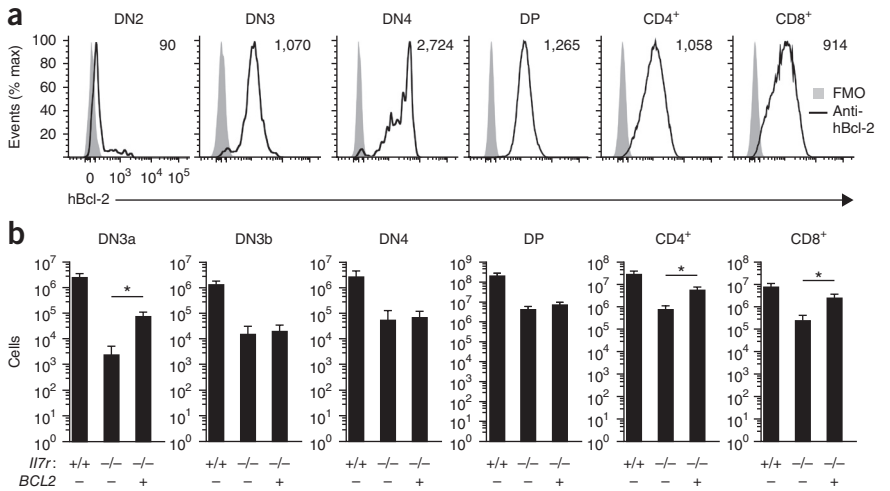

Figure 2 Human Bcl-2 fails to compensate for loss of IL-7 signaling during β-selection. (**a**) Flow cytometry of DN2, DN3 and DN4 thymocytes (gating, **Supplementary Fig. 1a**,**c**), as well as DP, CD4+ and CD8+ thymocyte subsets, from *Il7r*$^{-/-}$ mice expressing a transgene encoding human Bcl-2, stained with antibody to human Bcl-2 (hBcl-2) and plotted with the fluorescence-minus-one background control (numbers in plots as in **Fig. 1**). (**b**) Quantification of cells in each thymocyte subset (as in **a**) for *Il7r*$^{+/+}$ mice ($n = 4$) and *Il7r*$^{-/-}$ mice ($n = 9$) without expression of the human Bcl-2 transgene (*BCL2* –) and *Il7r*$^{-/-}$ mice expressing the transgene (*BCL2* +) ($n = 9$). *$P < 0.0001$ (Student's *t*-test). Data are representative of three independent experiments with similar results (**a**) or are pooled from three independent experiments (**b**; mean and s.d.)

and in all cells in subsequent stages (**Fig. 2a**). Although the number of DN3a cells was 30-fold higher in *Il7r*$^{-/-}$ mice expressing human Bcl-2 than in *Il7r*$^{-/-}$ mice, the number of cells in the DN3b, DN4 and DP compartments was not different in *Il7r*$^{-/-}$ mice expressing human Bcl-2 versus *Il7r*$^{-/-}$ mice (**Fig. 2b**). However, human Bcl-2 significantly increased the number of CD4+ and CD8+ SP thymocytes by sevenfold and tenfold, respectively (**Fig. 2b**). These findings identified a function for IL-7 signaling during β-selection *in vivo* that, in contrast to its function in earlier and later stages of T cell development, could not be recapitulated by Bcl-2.

Transcriptional responses to IL-7

The failure of human Bcl-2 to restore post-β-selection DN or DP thymocyte compartments in *Il7r*$^{-/-}$ mice suggested that IL-7 activates other pathways critical for β-selection *in vivo*. Therefore, we used gene-expression profiling to globally identify pathways rapidly regulated by IL-7 in DN3a, DN3b and DN4 cells. After 3 h of stimulation with IL-7, all three cell subsets showed robust induction of genes that are direct targets of the kinase Jak and STAT transcription factors (**Fig. 3**). This group included *Bcl2* and *Cish*, *Socs2* and *Socs3*, which encode feedback regulators of Jak-STAT signaling, as well as *Pim1* (which encodes the cell-survival mediator PIM1), *Tfrc* (which encodes CD71) and *Ccnd2* (which encodes the cell-cycle regulator CCND2). Thus, in addition to inducing genes encoding molecules involved in cell survival, IL-7 rapidly regulated the expression of genes encoding trophic receptors and cell-cycle regulators in pre- and post-β-selection DN thymocytes.

The response to stimulation with IL-7 was robust and complex in all three cell subsets (DN3a, DN3b and DN4), although the number of transcripts whose expression was significantly altered by IL-7 decreased substantially as DN3a cells matured into DN3b and DN4 cells (**Supplementary Fig. 2a**). Stimulation with Il-7 rapidly altered the expression of a large number of genes encoding molecules involved in signaling, translation, metabolism and cell growth (**Supplementary Fig. 2b**,**c** and **Supplementary Tables 1** and **2**). The nutrient transporter–encoding gene most potently induced was *Slc7a5* (**Supplementary Fig. 2c**); this encodes a transporter of large, neutral amino acids required for metabolic reprogramming during the activation and effector differentiation of T cells[22]. The signaling group included several genes encoding GTP-binding proteins, those encoding the GTPase Ras and mitogen-activated protein kinases, and those encoding the kinase PI(3)K and cell cycle regulator mTOR, as well as those encoding signaling receptors (**Fig. 3**). Finally, IL-7 increased the expression of genes encoding transcriptional regulators, most

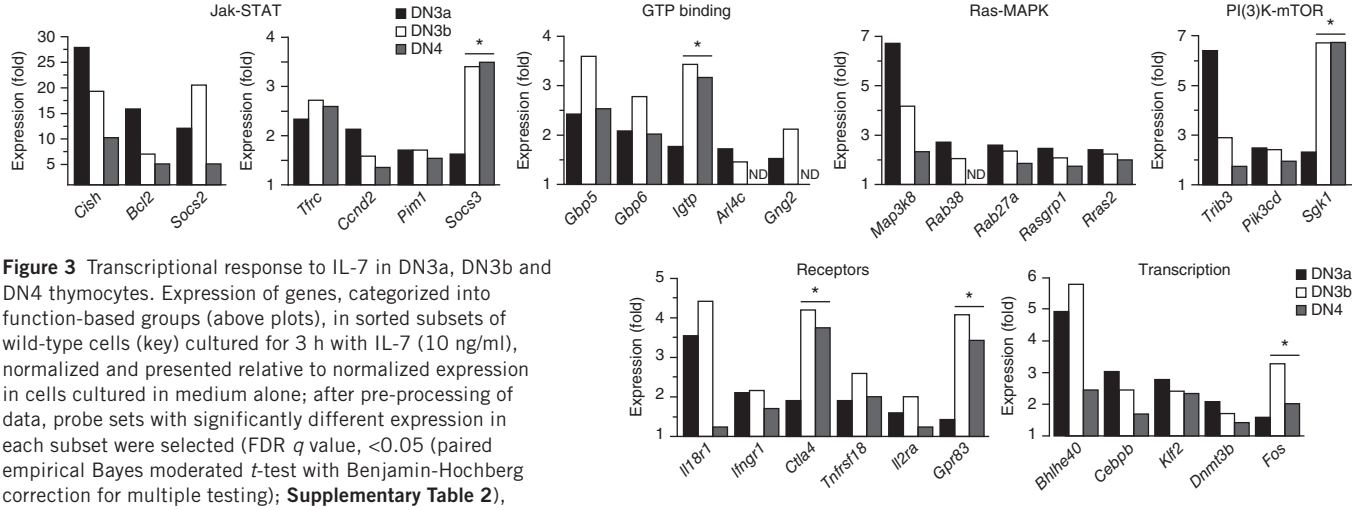

Figure 3 Transcriptional response to IL-7 in DN3a, DN3b and DN4 thymocytes. Expression of genes, categorized into function-based groups (above plots), in sorted subsets of wild-type cells (key) cultured for 3 h with IL-7 (10 ng/ml), normalized and presented relative to normalized expression in cells cultured in medium alone; after pre-processing of data, probe sets with significantly different expression in each subset were selected (FDR *q* value, <0.05 (paired empirical Bayes moderated *t*-test with Benjamin-Hochberg correction for multiple testing); **Supplementary Table 2**), then were collapsed into non-redundant gene lists. Asterisks indicate genes induced more robustly in post-selection DN3b and DN4 cells than in pre-selection DN3a cells. ND, not detected. Data are from one experiment with four biological replicates.

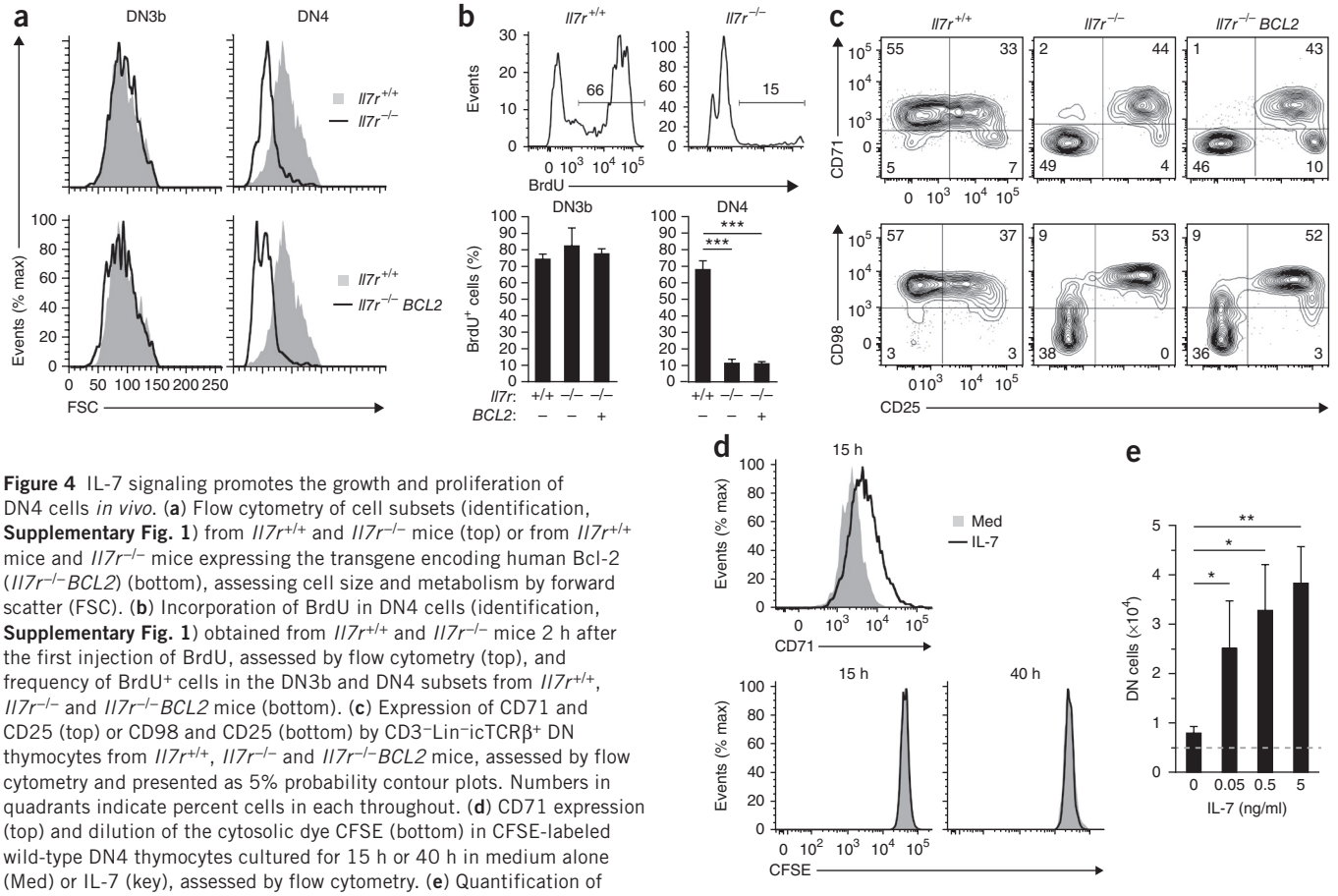

Figure 4 IL-7 signaling promotes the growth and proliferation of DN4 cells *in vivo*. (**a**) Flow cytometry of cell subsets (identification, **Supplementary Fig. 1**) from *Il7r*$^{+/+}$ and *Il7r*$^{-/-}$ mice (top) or from *Il7r*$^{+/+}$ mice and *Il7r*$^{-/-}$ mice expressing the transgene encoding human Bcl-2 (*Il7r*$^{-/-}$*BCL2*) (bottom), assessing cell size and metabolism by forward scatter (FSC). (**b**) Incorporation of BrdU in DN4 cells (identification, **Supplementary Fig. 1**) obtained from *Il7r*$^{+/+}$ and *Il7r*$^{-/-}$ mice 2 h after the first injection of BrdU, assessed by flow cytometry (top), and frequency of BrdU^{+} cells in the DN3b and DN4 subsets from *Il7r*$^{+/+}$, *Il7r*$^{-/-}$ and *Il7r*$^{-/-}$*BCL2* mice (bottom). (**c**) Expression of CD71 and CD25 (top) or CD98 and CD25 (bottom) by CD3^{-}Lin^{-}icTCRβ^{+} DN thymocytes from *Il7r*$^{+/+}$, *Il7r*$^{-/-}$ and *Il7r*$^{-/-}$*BCL2* mice, assessed by flow cytometry and presented as 5% probability contour plots. Numbers in quadrants indicate percent cells in each throughout. (**d**) CD71 expression (top) and dilution of the cytosolic dye CFSE (bottom) in CFSE-labeled wild-type DN4 thymocytes cultured for 15 h or 40 h in medium alone (Med) or IL-7 (key), assessed by flow cytometry. (**e**) Quantification of DN cells recovered from co-cultures of wild-type DN4 thymocytes (5×10^3 per well; dashed horizontal line) and OP9-DL4 cells cultured for 48 h in medium containing various concentrations of IL-7 (horizontal axis). *$P < 0.05$, **$P < 0.01$ and ***$P < 0.001$ (one-way analysis of variance (ANOVA) with Newman-Keuls post hoc *t*-test). Data are representative of three (**a**–**c**,**e**) or two (**d**) independent experiments with similar results (mean and s.d. of $n = 3$ biological (**b**) or technical (**e**) replicates per group in **b**,**e**).

notably *Bhlhe40* (**Fig. 3**), whose product is of unknown importance in T cell development. Although the magnitude and significance of IL-7-induced transcriptional changes were generally more robust in pre-selection DN3a cells than in DN3b or DN4 cells, some genes in each category were induced more in post-β-selection DN cells than in DN3a cells (**Fig. 3**), which suggested regulation cooperation with pre-TCR signaling.

IL-7 promotes growth and proliferation of DN4 cells

Since IL-7 significantly increased the expression of many genes encoding molecules that regulate metabolism, signaling and growth, we evaluated the effect of IL-7R deficiency on cell size, a reflection of cellular metabolism and proliferation during β-selection. Although the size of *Il7r*$^{+/+}$ DN3b cells was similar to that of *Il7r*$^{-/-}$ DN3b cells, *Il7r*$^{-/-}$ DN4 cells were much smaller than their *Il7r*$^{+/+}$ counterparts (**Fig. 4a**), which suggested loss of trophic signaling. Furthermore, IL-7 deficiency significantly impaired uptake of the thymidine analog BrdU by *Il7r*$^{-/-}$ DN4 cells but not its uptake by DN3b cells (**Fig. 4b**). Overexpression of *BCL2* did not prevent the atrophy of or restore the proliferation of *Il7r*$^{-/-}$ DN4 cells (**Fig. 4a**,**b**), which suggested that IL-7 signaling was needed to maintain the trophic responses and proliferation of DN4 thymocytes *in vivo* rather than simply to maintain Bcl-2-dependent survival.

DN3b and DN4 cells self-renew extensively in a pre-TCR-dependent fashion when cultured with OP9 stromal cells expressing Delta-like Notch ligands and with IL-7, and upregulation of the expression of trophic receptors such as CD71 and CD98 (a transporter of neutral amino acids) shows Notch dependence in such assays[8,23]. Because Notch signaling can regulate IL-7R expression in some contexts[24,25], the effects of Notch on trophic receptors could be mediated by IL-7. We therefore assessed the requirement for IL-7 signaling in inducing the expression of CD71 and CD98 during β-selection *in vivo*. As expected, *Il7r*$^{+/+}$ DN3b and DN4 cells were CD71^{hi}CD98^{hi} (**Fig. 4c**). In contrast, *Il7r*$^{-/-}$ DN4 cells lacked those trophic receptors, as well as the costimulatory receptors CD27 and CD28 and the cell surface marker CD24, although DN3b cells expressed normal amounts of these markers (data not shown). Once again, human Bcl-2 did not restore the expression of CD71 and CD98 in *Il7r*$^{-/-}$ DN4 cells (**Fig. 4c**). Although IL-7 increased CD71 expression in stromal cell–free cultures, it did not stimulate the proliferation of DN4 cells (**Fig. 4d**), which demonstrated that IL-7 signaling was unable to promote the self-renewal of DN4 cells without activation of Notch. Furthermore, Notch-induced proliferation of DN4 cells was dependent on IL-7 (**Fig. 4e**). Collectively, these experiments demonstrated that IL-7 signaling maintained the expression of nutrient receptors in DN4 cells and that Notch and IL-7 acted together to promote the self-renewal of DN4 cells.

IL-7 enforces the canonical DN3b-DN4-ISP sequence

DN4 cells are also referred to as 'pre-DP' cells because they rapidly generate DP progeny when cultured without stroma or cytokines[26].

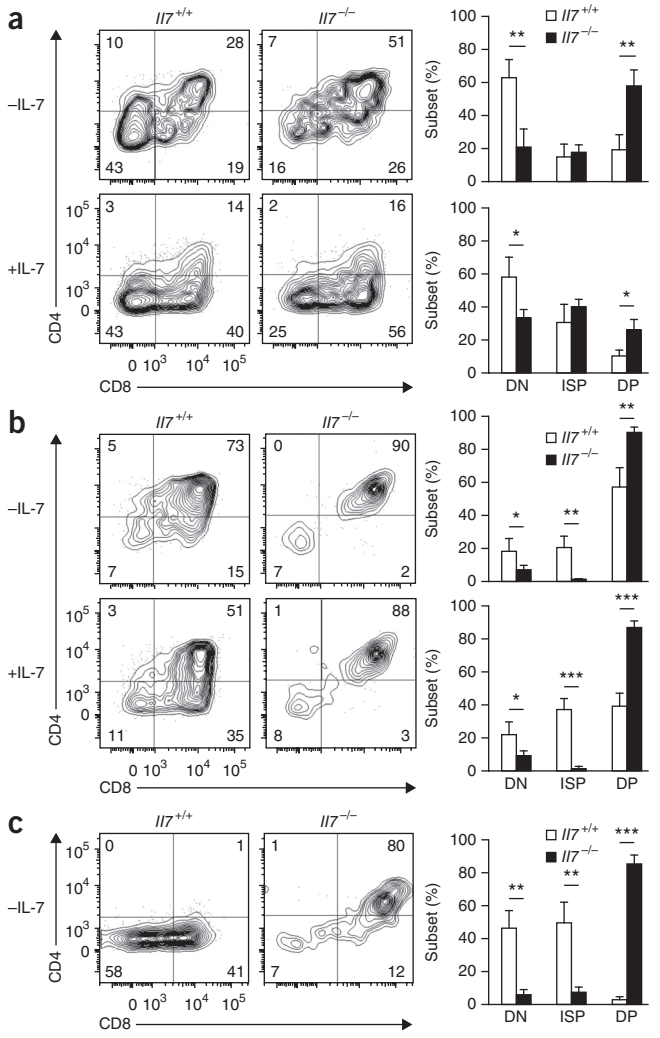

Figure 5 IL-7 signaling delays the differentiation of DN3b and DN4 cells into DP thymocytes. (**a**) Expression of CD4 versus CD8 in DN3b *Il7*$^{+/+}$ and *Il7*$^{-/-}$ cells cultured for 15 h in the absence of stromal cells with (+IL-7) or without (–IL-7) IL-7 (10 ng/ml), analyzed by flow cytometry (left), and quantification of cells in the DN (icTCRβ^{+}CD4^{-}CD8^{-}) subset, ISP (icTCRβ^{+}CD4^{-}CD8^{+}) subset or DP (icTCRβ^{+}CD4^{+}CD8^{+}) subset after culture (right). (**b**,**c**) Expression of CD4 versus CD8 in DN4 *Il7*$^{+/+}$ and *Il7*$^{-/-}$ cells cultured for 15 h as in **a** (**b**) or 5 h in medium alone (**c**), analyzed as in **a**. $^{*}P < 0.05$, $^{**}P \leq 0.01$ and $^{***}P < 0.0001$ (Student's *t*-test). Data are representative of at least three independent experiments with similar results (mean and s.d. of $n = 3$ (*Il7*$^{+/+}$) or 4 (*Il7*$^{-/-}$) technical replicates per group (**a**) or $n = 4$ (**b**) or 3 (**c**) technical replicates per genotype per group (**b**,**c**)).

Therefore, we evaluated the differentiation potential and kinetics of *Il7*$^{+/+}$ and *Il7*$^{-/-}$ DN3b and DN4 cells in stroma-free cultures with and without exogenous IL-7. Unexpectedly, after 15 h of culture without IL-7, *Il7*$^{-/-}$ DN3b cells generated significantly more DP progeny than did *Il7*$^{+/+}$ DN3b cells (**Fig. 5a**). However, both the DN progeny and ISP progeny of *Il7*$^{-/-}$ DN3b cells retained CD25 expression (**Supplementary Fig. 3a**), which suggested that the mutant DN3b cells generated ISP cells without obviously passing through the CD25^{-} DN4 stage. *Il7*$^{-/-}$ DN4 cells also generated significantly more DP progeny after 15 h than *Il7*$^{+/+}$ DN4 cells did (**Fig. 5b**), which demonstrated that they had enhanced capacity to develop into DP cells. Strikingly, most *Il7*$^{-/-}$ DN4 cells became DP within 5 h and seemed to not pass through the ISP stage, whereas *Il7*$^{+/+}$ DN4 cells generated only ISP cells during this time (**Fig. 5c**). The addition of IL-7 to DN3b cells also increased the frequency of ISP cells at the expense of the generation of DP cells, but this effect of IL-7 was significant only for *Il7*$^{-/-}$ DN3b cells ($P < 0.001$; **Supplementary Fig. 3b**). IL-7 also increased the frequency of ISP cells in cultures of *Il7*$^{+/+}$ DN4 cells but not in cultures of *Il7*$^{-/-}$ DN4 cells (**Fig. 5b** and **Supplementary Fig. 3b**), which indicated that *Il7*$^{-/-}$ DN4 cells, in contrast to *Il7*$^{+/+}$ DN4 cells, were insensitive to IL-7. Collectively, these experiments suggested that *Il7*$^{-/-}$ DN3b cells generated ISP and DP progeny without obviously passing through the DN4 stage, whereas *Il7*$^{-/-}$ DN4 cells rapidly generated DP progeny without obviously passing through the ISP stage.

Deletion of *Bcl6* improves the self-renewal of DN4 cells

We noted that *Bcl6* was the gene most significantly downregulated after treatment of DN3a, DN3b and DN4 cells with IL-7, with false-discovery rate (FDR)-adjusted *q* values of 1×10^{-18}, 4.2×10^{-20} and 2×10^{-12}, respectively (**Fig. 6a** and **Supplementary Table 2**). Furthermore, DN3b and DN4 cells from *Il7*$^{-/-}$ mice expressed significantly more *Bcl6* mRNA than did their *Il7*$^{+/+}$ counterparts (**Fig. 6a**), which suggested loss of IL-7-mediated repression. Notably, thymocytes substantially upregulate *Bcl6* expression as proliferation ceases during the DN3-to-DP transition (as reported by the Immunological Genome Project), but the functions of Bcl-6 in T cell development have not yet been identified. Therefore, we investigated whether IL-7-induced repression of *Bcl6* in DN4 cells was important for differentiation and self-renewal during β-selection. Because *Bcl6*$^{-/-}$ mice develop a lethal inflammatory disease[27,28], we generated DN4 thymocytes by culturing *Bcl6*$^{+/+}$ or *Bcl6*$^{-/-}$ fetal liver hematopoietic progenitor cells together with OP9 stromal cells expressing Delta-like ligand 4 (OP9-DL4 cells). We found that *Bcl6*$^{+/+}$ and *Bcl6*$^{-/-}$ DN4 cells sorted from these co-cultures generated a similar frequency of ISP and DP cells after culture with or without IL-7 (**Fig. 6b**), which suggested that Bcl-6 did not obviously regulate differentiation during β-selection. However, *Bcl6* deficiency increased the recovery of DN4 cells in the absence of IL-7 compared with the recovery for wild-type cells cultured without IL-7 (**Fig. 6c**), compared with the recovery for wild-type cells cultured without IL-7 which suggested that repression of *Bcl6* was a major mechanism by which IL-7 induced the self-renewal of DN4 cells. Nonetheless, the addition of IL-7 further augmented the proliferation of *Bcl6*$^{-/-}$ DN4 cells (**Fig. 6c**), which suggested that deletion of *Bcl6* did not fully recapitulate the proliferation-inducing functions of IL-7.

Effect of IL-7 on ISP thymocytes

We also investigated the generation of ISP cells in the absence of IL-7 signaling *in vivo*. The number of ISP cells (defined as in **Supplementary Fig. 4a**) was 100-fold lower in *Il7r*$^{-/-}$ mice than in *Il7r*$^{+/+}$ mice (**Fig. 7a**), in keeping with the diminished pools of all earlier progenitor cells (**Fig. 2b**). However, in contrast to *Il7r*$^{-/-}$ DN4 cells, *Il7r*$^{-/-}$ ISP cells were large CD71^{hi}CD98^{hi} cells, similar to wild-type ISP cells (**Supplementary Fig. 4b**). Expression of CD71 and CD98 in eDP and lDP cells also persisted in the absence of IL-7 signaling (**Supplementary Fig. 4c**). *Il7*$^{+/+}$ and *Il7*$^{-/-}$ ISP cells generated DP progeny *in vitro* with similar kinetics (**Fig. 7b**), which suggested that IL-7 deficiency did not affect the ISP-to-DP transition. Thus, although loss of IL-7 signaling impaired the trophic responses of DN4 cells and accelerated their differentiation, it did not affect these functions in ISP or DP cells. Nonetheless, *Il7r*$^{-/-}$ ISP cells generated *in vivo* (**Fig. 7a**) and *in vitro* (**Supplementary Fig. 3a**) did express CD25 (normally

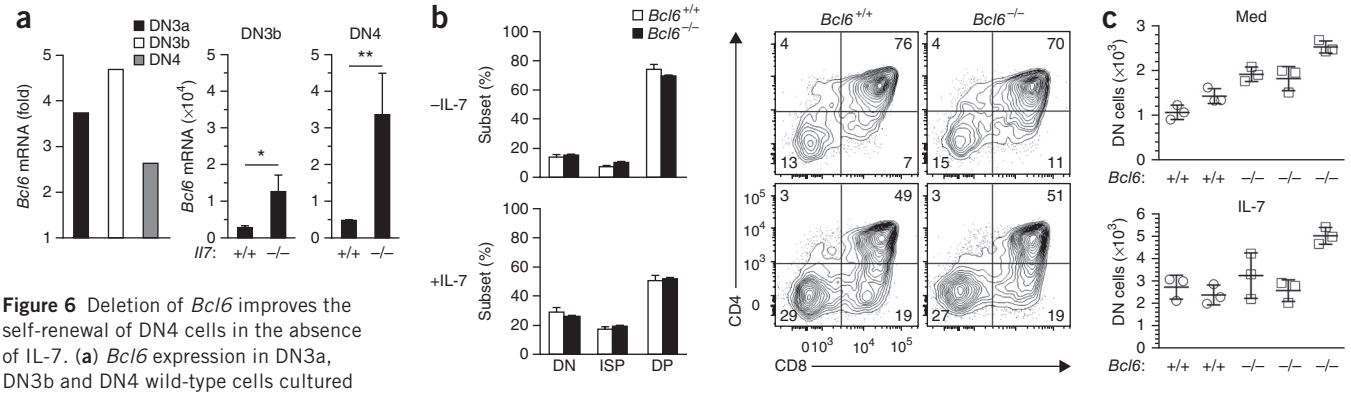

Figure 6 Deletion of *Bcl6* improves the self-renewal of DN4 cells in the absence of IL-7. (**a**) *Bcl6* expression in DN3a, DN3b and DN4 wild-type cells cultured in IL-7, presented relative to its expression in their counterparts cultured in medium alone (as in **Fig. 3**; FDR-adjusted *q* values, **Supplementary Table 2**) (left), and quantitative RT–PCR analysis of *Bcl6* mRNA in DN3b and DN4 $Il7^{+/+}$ and $Il7^{-/-}$ thymocytes, normalized to results obtained for *Cd45* mRNA. (**b**) Quantification of cells in the DN, ISP and DP subsets (as in **Fig. 5a**) among the progeny of DN4 cells sorted from co-cultures of $Bcl6^{+/+}$ and $Bcl6^{-/-}$ fetal liver hematopoietic progenitor cells cultured for 9 d with OP9-DL4 cells, then re-cultured (after sorting) for 48 h with or without IL-7 (left), and expression of CD4 versus CD8 by the sorted DN4 cells cultured with or without IL-7 (right), analyzed by flow cytometry (right). (**c**) Quantification of DN cells among the progeny of sorted DN4 cells in **b** cultured without or with IL-7. Each symbol represents an independent OP9 culture from two $Bcl6^{+/+}$ or three $Bcl6^{-/-}$ individual fetuses; small horizontal lines indicate the mean (±s.d.). $^{**}P < 0.0001$, $^{*}P \leq 0.01$ (Student's *t*-test (**a**)). Data are representative of two experiments with similar results (mean and s.d. of $n = 3$ technical replicates per group in **a**) or one experiment (**b**,**c**; mean and s.d. of $n = 2$ ($Bcl6^{+/+}$) or 3 ($Bcl6^{-/-}$) fetuses (three replicate cultures each)).

not expressed by these cells), which suggested that in the absence of IL-7 signaling, most ISP cells seemed to arise directly from CD25⁺ DN3b cells rather than from CD25⁻ DN4 cells.

To directly evaluate the DN3b-to-DP transition *in vivo*, we monitored the differentiation of proliferating cells in $Il7r^{-/-}$ and $Il7r^{+/+}$ mice at various times after injection of BrdU. As expected, DN3a cells from both genotypes of mice were quiescent (mostly BrdU⁻) 2 h after injection of BrdU but accumulated the label from proliferating precursor cells over the next 24–48 h (**Fig. 7c**). Thus, the absence of intrathymic IL-7 signaling did not affect the generation of DN3a cells from proliferating precursor cells but greatly decreased the survival of DN3a cells (**Fig. 2**). In contrast to quiescent DN3a cells, 65–75% of wild-type DN3b, DN4 and ISP cells were BrdU⁺ after 2 h (**Fig. 7d**), which confirmed that each subset was rapidly cycling. The frequency of labeled DN3b cells decreased after 24 h (**Fig. 7d**), consistent with derivation from quiescent DN3a precursor cells, whereas DN4 cells and ISP cells had substantial labeling (**Fig. 7d**), consistent with their derivation from cycling DN3b precursor cells and DN4 precursor cells, respectively. As shown above (**Fig. 4**), only ~10% of $Il7r^{-/-}$ DN4 cells were BrdU⁺ 2 h after injection (**Fig. 7d**). However, 70–90% of $Il7r^{-/-}$ DN3b cells were BrdU⁺ (**Fig. 7d**), which suggested that most DN4 cells were derived from quiescent DN3a cells rather than from cycling DN3b cells in *Il7r* mutant mice. Indeed, BrdU accumulated in $Il7r^{-/-}$ DN4 cells slowly over the next 2 d, similar to its accumulation in both $Il7r^{+/+}$ DN3a cells and $Il7r^{-/-}$ DN3a cells (**Fig. 7d**). Furthermore, $Il7r^{-/-}$ ISP cells

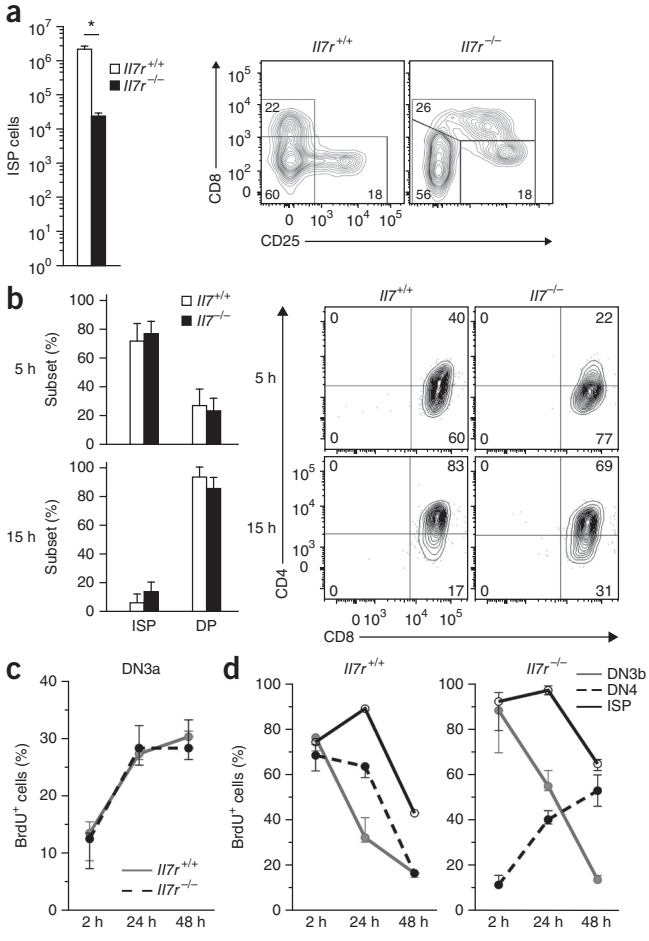

Figure 7 $Il7r^{-/-}$ DN4 thymocytes are not the precursors of the ISP cell subset. (**a**) Quantification of ISP ($CD3^{-}CD24^{+}$) cells in the $Lin^{-}CD4^{-}CD8^{+}icTCR\beta^{+}$ subset (**Supplementary Fig. 4a**) of thymocytes from $Il7^{+/+}$ mice ($n = 4$) and $Il7r^{-/-}$ mice ($n = 6$), analyzed by flow cytometry (left), and expression of CD8 versus CD25 by thymocytes gated on $Lin^{-}CD3^{-}CD4^{-}icTCR\beta^{+}$ cells (right). Numbers in outlined areas (right) indicate percent $CD8^{+}CD25^{neg-pos}$ (ISP) cells (top left), $CD8^{neg-lo}CD25^{-}$ (DN4) cells (bottom left) or $CD8^{neg-lo}CD25^{+}$ (DN3b) cells. (**b**) Quantification of ISP and DP cells among sorted ISP $Il7^{+/+}$ and $Il7r^{-/-}$ cells cultured for 5 h (top) or 15 h (bottom) without IL-7, analyzed by flow cytometry (as in **Fig. 5**) (left), and expression of CD4 versus CD8 by the cells at left (right). (**c**,**d**) Frequency of BrdU⁺ thymocytes in the DN3a subset (**c**) or DN3b, DN4 and ISP subsets (**d**) obtained from $Il7r^{+/+}$ and $Il7r^{-/-}$ mice at 2, 24 and 48 h after injection of BrdU and analyzed by flow cytometry (data for 2 h in **Fig. 4b** replotted here). $^{*}P < 0.0001$ (Student's *t*-test). Data are representative of three (**a**,**b**) or two (**c**,**d**) independent experiments with similar results (mean and s.d. in **a**; mean and s.d. of $n = 3$ technical (**b**) or biological (**c**,**d**) replicates per time point per genotype in **b**–**d**).

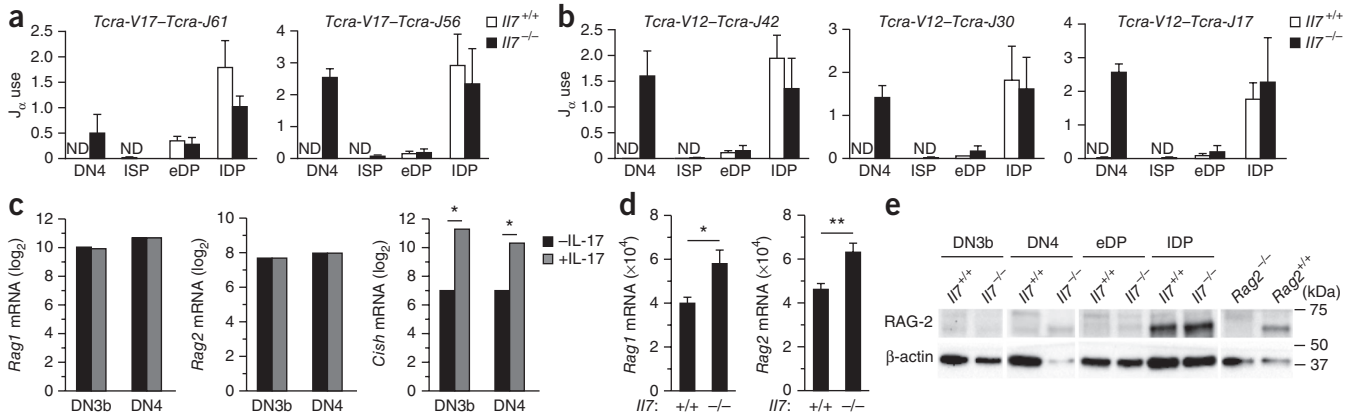

Figure 8 IL-7 signaling prevents premature recombination of the *Tcra* locus in the DN4 subset. (**a**,**b**) Quantitative PCR analysis of recombination of the loci encoding V_α and J_α in genomic DNA from DN4, ISP, eDP ($CD71^{hi}FSC^{hi}$) and IDP ($CD71^{lo}FSC^{lo}$) thymocytes, analyzed with primers for sequence encoding $V_\alpha17$ (*Tcra-V17*) and proximal segments encoding $J_\alpha61$ (*Tcra-J61*) or $J_\alpha56$ (*Tcra-J56*) (**a**), or sequence encoding $V_\alpha12$ (*Tcra-V12*; primers detect multiple, widely distributed members of this family) and central segments encoding $J_\alpha42$ (*Tcra-J42*) or $J_\alpha30$ (*Tcra-J30*) or a distal segment encoding $J_\alpha17$ (*Tcra-J17*) (**b**), presented (as J_α use) relative to that in unfractionated wild-type thymocytes. (**c**) Expression of *Rag1*, *Rag2* and *Cish* in DN3b and DN4 cells cultured with or without IL-17 (10 ng/ml) (from **Fig. 3**; *FDR-adjusted *q* value, <0.0001). (**d**) Quantitative RT-PCR analysis of *Rag1* and *Rag2* mRNA in sorted DN4 $Il7^{+/+}$ and $Il7^{-/-}$ thymocytes, normalized to results obtained for *Cd45*. $*P < 0.01$ and $**P < 0.0001$ (Student's *t*-test). (**e**) Immunoblot analysis of RAG-2 and β-actin (loading control) in subsets from $Il7^{+/+}$ and $Il7^{-/-}$ thymuses, as well as extracts from total $Rag2^{+/+}$ and $Rag2^{-/-}$ thymocytes (positive control and negative control, respectively). Data are representative of two or more independent experiments with similar results (**a**,**b**; mean and s.d. of $n = 4$ (two biological replicates per subset per genotype and two technical replicates per sort)), one experiment with four biological replicates (**c**), one experiment (**d**; mean and s.d. of $n = 3$ technical replicates per group) or three independent experiments with similar results (**e**).

had undergone considerable labeling after 24 h (**Fig. 7d**), which suggested that they were not derived from quiescent DN4 cells but instead were derived directly from cycling DN3b cells.

Effect of IL-7 on *Tcra* recombination

Primary recombination of the gene encoding TCRα involving 3′ gene segments encoding V_α and 5′ gene segments encoding J_α normally initiates in eDP cells as they become quiescent lDP cells, with secondary recombination events that use more distal gene segments occurring exclusively in non-cycling lDP cells[10,29]. Since DN4 cells generated in the absence of IL-7 were abnormally quiescent, we investigated whether they had undergone premature *Tcra* recombination. We sorted DN4, ISP, eDP and lDP thymocytes from $Il7^{-/-}$ and $Il7^{+/+}$ mice and used quantitative PCR to quantify primary rearrangements of *Tcra* involving 3′ segments encoding $V_\alpha17$ and 5′ segments encoding $J_\alpha61$ and $J_\alpha56$, as well as secondary rearrangements involving more 5′ segments encoding $V_\alpha12$ and 3′ segments encoding $J_\alpha42$, $J_\alpha30$ and $J_\alpha17$.

As expected, we detected very small amounts of primary and secondary rearrangements of *Tcra* in cycling $Il7^{+/+}$ DN4, ISP and $CD71^+$ $CD98^+$ eDP cells, whereas we detected large amounts of both primary and secondary rearrangements in post-mitotic $CD71^-CD98^-$ lDP cells of each genotype (**Fig. 8a**,**b**). In contrast, $Il7^{-/-}$ DN4 cells had abundant primary and secondary rearrangements that were similar in frequency to those found in $Il7^{+/+}$ lDP cells (**Fig. 8a**,**b**). Thus, abnormally quiescent DN4 cells from IL-7-deficient mice underwent premature and extensive recombination of *Tcra*. Nonetheless, $Il7^{-/-}$ ISP and eDP cells had very small amounts of both primary rearrangements and secondary rearrangements of *Tcra*, similar to the amounts seen in $Il7^{+/+}$ ISP and eDP cells (**Fig. 8a**,**b**). Furthermore, we did not detect *Tcra* rearrangements in $Il7^{-/-}$ DN3b cells (data not shown). The contrast between quiescent DN4 cells and cycling ISP and eDP cells from $Il7^{-/-}$ mice in their *Tcra*-rearrangement status provided further evidence that the DN4 cells were not precursors of ISP and eDP cells in these mutant mice.

The extensive rearrangement of *Tcra* in $Il7^{-/-}$ DN4 cells suggested that they prematurely upregulated their expression of *Rag1* and *Rag2*. However, our gene-expression-profiling experiments showed that treatment for 3 h with IL-7 did not rapidly decrease the expression of *Rag1* and *Rag2* in DN3b or DN4 thymocytes, in contrast to the expression of direct targets of STAT5, such as *Cish* (**Fig. 8c**) and *Bcl6* (**Fig. 6a**). Thus, *Rag1* and *Rag2* did not seem to be direct transcriptional targets of IL-7 in DN thymocytes. Nonetheless, the abundance of *Rag1* and *Rag2* mRNA was significantly higher in DN4 cells isolated from $Il7^{-/-}$ mice than in those from $Il7^{+/+}$ mice (**Fig. 8d**), which probably reflected the accelerated differentiation of these cells in the absence of IL-7. Notably, RAG-2 undergoes proteolysis mediated by cyclin A and its associated kinase CDK2 during S phase of the cell cycle to minimize the oncogenic potential of RAG-induced DNA breaks in cycling cells[30]. Since IL-7-deficient DN4 cells were abnormally quiescent, we also evaluated the abundance of RAG-2 by immunoblot analysis. As expected, RAG-2 expression was low in cycling DN3b and eDP cells but was high in quiescent lDP cells in both $Il7^{+/+}$ mice and $Il7^{-/-}$ mice (**Fig. 8e**). In contrast, RAG-2 was barely detectable in cycling DN4 cells from $Il7^{+/+}$ mice but was readily detectable in quiescent DN4 cells from $Il7^{-/-}$ mice, even though the low abundance of DN4 cells in $Il7^{-/-}$ mice necessitated underloading of this lane (**Fig. 8e**). Notably, RAG-2 expression was not elevated in cycling DN3b cells from $Il7^{-/-}$ mice (**Fig. 8e**), which suggested that loss of IL-7 signaling was not sufficient to increase RAG-2 in cycling cells. Collectively, these data suggested that IL-7 deficiency promoted premature re-expression of *Rag1* and *Rag2* and rearrangement of *Tcra* by preventing cycling and accelerating the differentiation of DN4 cells (**Supplementary Fig. 5**).

DISCUSSION

Our study has demonstrated that the absence of intrathymic IL-7 signaling caused several abnormalities during β-selection that were not ameliorated by transgenic expression of *BCL2*. During β-selection in wild-type mice, the canonical differentiation sequence is linear: DN3a-DN3b-DN4-ISP-eDP-lDP. In contrast, we have provided *in vitro* and *in vivo* evidence that DP cells arose via two abnormal pathways in IL-7-mutant mice. In one pathway, DN3a cells generated

DN4 cells that prematurely upregulated *Bcl6*, failed to self-renew and rapidly differentiated into lDP cells without obviously passing through the ISP stage. IL-7-deficient quiescent DN4 cells also prematurely re-expressed *Rag1* and *Rag2*, which allowed premature primary and secondary recombination of *Tcra*. However, there was also a 'cycling' pathway in which some DN3a cells generate cycling DN3b progeny that differentiated into DP cells via ISP intermediates that expressed CD25 and thus did not seem to transit through the DN4 stage. The abnormal retention of CD25 expression by proliferating post-β-selection cells in IL-7-mutant mice might suggest abnormal persistence of Notch signaling, since *Il2ra* (which encodes CD25) is a direct target of Notch in DN thymocytes[31]. Interestingly, IL-7 increased the frequency of ISP cells when added to $Il7^{+/+}$ DN3b and DN4 cells or to $Il7^{-/-}$ DN3b cells. Since ISP cells do not express IL-7R[18], IL-7 acts on DN3b and/or DN4 cells to enhance the generation of ISP cells and/or delay their differentiation into DP cells. Thus, IL-7 signaling in DN3 and DN4 cells may delay some aspects of differentiation during the DN3b-to-DP transition. Collectively these findings demonstrate that IL-7 signaling is needed to maintain the self-renewal of DN4 cells, to enforce the canonical DN3a-DN3b-DN4-ISP-DP differentiation sequence and to delay *Tcra* rearrangement until after proliferation ceases during thymocyte β-selection.

In agreement with a published study[21], we found that IL-7R expression was higher in DN3b cells that had received signaling via the pre-TCR than in DN3a cells. However, in contrast to studies examining total DN3 and DN4 cells[19], we found that IL-7 robustly induced the phosphorylation of STAT5 and significantly increased the abundance of *Bcl2* mRNA in icTCRβ$^+$ DN3b and DN4 thymocytes *in vitro*. Furthermore, we showed that IL-7 induced the phosphorylation of STAT5 and maintained the levels of mouse Bcl-2 protein in DN3b and DN4 cells *in vivo*. Although a published study concluded that IL-7 is needed to maintain the survival but not the proliferation of fetal DN4 thymocytes[21], we found that overexpression of human Bcl-2 in $Il7^{-/-}$ mice did not restore DN3b, CD4, CD8 ISP or DP cells, despite its significant restoration of the DN3a and CD4$^+$ or CD8$^+$ SP subsets. While we cannot rule out the possibility that IL-7 functions differ in fetal DN4 cells versus adult DN4 cells, our findings demonstrated that in addition to signaling via the pre-TCR and Notch1, IL-7 signaling was maintained during β-selection *in vivo* and had functions that could not be recapitulated by Bcl-2.

Our study suggested that IL-7 signaling was needed to prevent the atrophy of DN4 cells and maintain their proliferation *in vivo*. Furthermore, IL-7 greatly enhanced the Notch-dependent self-renewal of DN4 cells *in vitro*. We identified several mechanisms underlying the trophic and pro-proliferative functions of IL-7 during β-selection. First, IL-7 maintained expression of the nutrient receptors CD71 and CD98 in DN4 thymocytes, which has been reported as being Notch dependent *in vitro*[8,23]. However, Notch activity sustains IL-7R expression in some contexts[24,25], so the effect of Notch on the expression of CD71 and CD98 might have been indirect. Indeed, treatment with IL-7 alone increased the expression of *Cd71* mRNA and CD71 protein in DN4 thymocytes but was not sufficient to induce the proliferation of DN4 cells in the absence of Notch activity. Therefore, our data suggested that IL-7 acted together with Notch1 to maintain the expression of nutrient receptors in and proliferation of DN4 thymocytes. Second, IL-7 induced the expression of genes encoding an unexpectedly complex array of cell-growth regulators in DN thymocytes, including metabolic enzymes, translational regulators and nutrient transporters. Most genes were more potently induced in pre-selection DN3a cells than in DN3b and DN4 cells, which suggested that the profound effect of IL-7 during β-selection could have been partly due to changes induced before pre-TCR expression. Nonetheless, a small group of genes were more potently induced in post-selection DN thymocytes than in other cells, which suggested that they may have been cooperatively regulated by signaling via the pre-TCR plus signaling via IL-7. Finally, deletion of *Bcl6* partially restored the self-renewal of DN4 cells in the absence of IL-7, which indicated that repression of *Bcl6* is an important function of IL-7 during β-selection. Although Bcl-6 promotes the self-renewal of pre-B cells by limiting p53-induced apoptosis[15], overexpression of human Bcl-2 did not restore DN4 cellularity in IL-7R-deficient mice. Thus, Bcl-6 probably limits the self-renewal of DN4 cells by inhibiting proliferation, perhaps by repressing the gene encoding the cell-cycle regulator c-Myc[32] rather than by simply promoting survival. Overall, our data suggest that during β-selection, IL-7 acts together with signaling via the pre-TCR and receptors of the Notch family to reprogram metabolism and translation to meet the biosynthetic demands of clonal expansion by inducing the expression of genes encoding a large number of metabolic regulators and repressing *Bcl6*. This prominent role for IL-7 in regulating the metabolism and proliferation of precursors of T cells probably explains why this *Il7r* and downstream genes are frequently mutated in T cell leukemia[33].

Among the cell-growth regulators induced by IL-7, regulators of the PI(3)K-mTOR signaling pathway are probably particularly important for β-selection. The importance of PI(3)K signaling in β-selection was first revealed by the observation that deletion of *Pten*, which encodes a lipid phosphatase that counteracts PI(3)K function, greatly restores the DP thymocyte pool in mice with mutations that compromise signaling via the pre-TCR or IL-7R[34]. *Pik3cd* encodes the PI(3)K isoform required for β-selection[35], and its expression was rapidly enhanced by IL-7 in both pre-β-selection thymocytes and post-β-selection thymocytes, suggestive of a positive feedback loop. The action of PI(3)K leads to activation of the kinase Akt and signaling via mTOR to increase nutrient uptake and metabolism during proliferation. However, the serum- and glucocorticoid-induced kinase SGK, rather than Akt, may control cell growth and metabolism downstream of mTOR signaling[36]. Since *Sgk1* (which encodes SGK) was induced more by IL-7 in DN3b and DN4 cells than in DN3a cells, this kinase might have particularly important roles in inducing the clonal expansion of pre-TCR$^+$ cells.

Although signaling via the pre-TCR is thought to activate the enhancer E_α as early as the DN4 stage[12,37,38], in IL-7-sufficient mice, very little recombination of *Tcra* occurred until the DP stage. However, $Il7^{-/-}$ DN4 cells had large amounts of primary and secondary rearrangements of *Tcra*, similar to the amounts in $Il7^{+/+}$ lDP cells, which indicated that IL-7 signaling might normally prevent *Tcra* rearrangement in DN4 thymocytes. Several possible mechanisms might underlie this role of IL-7. During B cell development, IL-7-induced STAT5 tetramers directly repress the transcription and rearrangement of the locus encoding immunoglobulin κ-chain via an epigenetic mechanism[13,14]. However, E_α does not contain consensus STAT5-binding sites, although several low-stringency motifs are present (data not shown). Furthermore, a mechanism that involves active IL-7-induced repression of *Tcra* rearrangement does not readily explain the differences in the abundance of *Tcra* rearrangements in $Il7^{-/-}$ DN4 and lDP cells relative to that in $Il7^{-/-}$ ISP and eDP cells.

During B cell development, signaling via the pre-BCR and signaling via IL-7 act together to downregulate expression of *Rag1* and *Rag2* by inhibiting transcriptions factors of the Foxo family, thus preventing variable-diversity-joining (V(D)J) recombination during pre-BCR-induced clonal expansion[39–41]. In contrast, IL-7 did not induce rapid changes in the expression of *Rag1* and *Rag2* in post-β-selection thymocytes

in our study. Nonetheless, DN4 cells generated in IL-7-deficient mice had higher steady mRNA levels, which probably reflected their accelerated differentiation kinetics. We also documented that non-cycling DN4 thymocytes from IL-7-deficient mice had higher expression of RAG-2 protein than did cycling DN4 cells from IL-7-sufficient mice, consistent with decreased proteolysis of RAG-2 mediated by cyclin A and CDK2 (ref. 30). Therefore, our data suggested that IL-7 indirectly inhibited *Tcra* rearrangement by promoting the proliferation of DN4 cells and degradation of RAG-2 rather than by directly repressing the expression of *Rag1* and *Rag2*. Collectively, our study has shown that thymocyte β-selection is orchestrated by a complex interplay of signaling via the pre-TCR, Notch and IL-7R.

METHODS

Methods and any associated references are available in the online version of the paper.

Accession codes. GEO: microarray data, GSE63932.

Note: Any Supplementary Information and Source Data files are available in the online version of the paper.

ACKNOWLEDGMENTS

We thank R. Gerstein (University of Massachusetts) for *Il7*$^{-/-}$ mice; and R. Dalla-Favera (Columbia University) for *Bcl6*$^{+/-}$ mice. Microarray analyses were performed at The Centre for Applied Genomics, Hospital for Sick Children with support from Genome Canada/Ontario Genomics Institute and the Canada Foundation for Innovation; flow cytometry was performed at The SickKids-UHN Flow Cytometry Facility, supported by the Ontario Institute for Cancer Research, the McEwen Centre for Regenerative Medicine, the Canada Foundation for Innovation and the SickKids Foundation. Supported by the Canadian Institutes of Health Research (FRN 11530 to C.J.G.), the US National Institutes of Health (R37 GM41052 to M.S.K.), the National Center for Research Resources of the US National Institutes of Health (P41 GM103504 to G.D.B.).

AUTHOR CONTRIBUTIONS

A.B., I.R.M., H.-Y.S., G.B., J.S.Y., S.G.C., B.M. and P.E.K. designed, performed and analyzed experiments; V.V., S.B. and G.D.B. performed statistical analysis and gene set–enrichment analysis of Illumina gene-expression data; A.B., H.-Y.S. and M.S.K. wrote the manuscript; and C.J.G. analyzed data, supervised the study and wrote the manuscript.

COMPETING FINANCIAL INTERESTS

The authors declare no competing financial interests.

1. Yuan, J.S., Kousis, P.C., Suliman, S., Visan, I. & Guidos, C.J. Functions of notch signaling in the immune system: consensus and controversies. *Annu. Rev. Immunol.* **28**, 343–365 (2010).
2. Mazzucchelli, R. & Durum, S.K. Interleukin-7 receptor expression: intelligent design. *Nat. Rev. Immunol.* **7**, 144–154 (2007).
3. Akashi, K., Kondo, M., von Freeden-Jeffry, U., Murray, R. & Weissman, I.L. Bcl-2 rescues T lymphopoiesis in interleukin-7 receptor-deficient mice. *Cell* **89**, 1033–1041 (1997).
4. Maraskovsky, E. *et al.* Bcl-2 can rescue T lymphocyte development in interleukin-7 receptor-deficient mice but not in mutant rag-1–/– mice. *Cell* **89**, 1011–1019 (1997).
5. Khaled, A.R. *et al.* Bax deficiency partially corrects interleukin-7 receptor α deficiency. *Immunity* **17**, 561–573 (2002).
6. Pellegrini, M. *et al.* Loss of Bim increases T cell production and function in interleukin 7 receptor-deficient mice. *J. Exp. Med.* **200**, 1189–1195 (2004).
7. Guidos, C.J. Synergy between the pre-T cell receptor and Notch: cementing the alphabeta lineage choice. *J. Exp. Med.* **203**, 2233–2237 (2006).
8. Kelly, A.P. *et al.* Notch-induced T cell development requires phosphoinositide-dependent kinase 1. *EMBO J.* **26**, 3441–3450 (2007).
9. Yannoutsos, N. *et al.* The role of recombination activating gene (RAG) reinduction in thymocyte development *in vivo*. *J. Exp. Med.* **194**, 471–480 (2001).
10. Seitan, V.C. *et al.* A role for cohesin in T-cell-receptor rearrangement and thymocyte differentiation. *Nature* **476**, 467–471 (2011).
11. Shih, H.Y., Hao, B. & Krangel, M.S. Orchestrating T-cell receptor alpha gene assembly through changes in chromatin structure and organization. *Immunol. Res.* **49**, 192–201 (2011).
12. del Blanco, B., Garcia-Mariscal, A., Wiest, D.L. & Hernandez-Munain, C. Tcra enhancer activation by inducible transcription factors downstream of pre-TCR signaling. *J. Immunol.* **188**, 3278–3293 (2012).
13. Malin, S. *et al.* Role of STAT5 in controlling cell survival and immunoglobulin gene recombination during pro-B cell development. *Nat. Immunol.* **11**, 171–179 (2010).
14. Mandal, M. *et al.* Epigenetic repression of the Igk locus by STAT5-mediated recruitment of the histone methyltransferase Ezh2. *Nat. Immunol.* **12**, 1212–1220 (2011).
15. Duy, C. *et al.* BCL6 is critical for the development of a diverse primary B cell repertoire. *J. Exp. Med.* **207**, 1209–1221 (2010).
16. Walker, S.R., Nelson, E.A. & Frank, D.A. STAT5 represses BCL6 expression by binding to a regulatory region frequently mutated in lymphomas. *Oncogene* **26**, 224–233 (2007).
17. Basso, K. & Dalla-Favera, R. BCL6: master regulator of the germinal center reaction and key oncogene in B cell lymphomagenesis. *Adv. Immunol.* **105**, 193–210 (2010).
18. Yu, Q., Erman, B., Park, J.H., Feigenbaum, L. & Singer, A. IL-7 receptor signals inhibit expression of transcription factors TCF-1, LEF-1, and RORγt: impact on thymocyte development. *J. Exp. Med.* **200**, 797–803 (2004).
19. Van De Wiele, C.J. *et al.* Thymocytes between the β-selection and positive selection checkpoints are nonresponsive to IL-7 as assessed by STAT-5 phosphorylation. *J. Immunol.* **172**, 4235–4244 (2004).
20. Balciunaite, G., Ceredig, R., Fehling, H.J., Zuniga-Pflucker, J.C. & Rolink, A.G. The role of Notch and IL-7 signaling in early thymocyte proliferation and differentiation. *Eur. J. Immunol.* **35**, 1292–1300 (2005).
21. Trigueros, C. *et al.* Pre-TCR signaling regulates IL-7 receptor alpha expression promoting thymocyte survival at the transition from the double-negative to double-positive stage. *Eur. J. Immunol.* **33**, 1968–1977 (2003).
22. Sinclair, L.V. *et al.* Control of amino-acid transport by antigen receptors coordinates the metabolic reprogramming essential for T cell differentiation. *Nat. Immunol.* **14**, 500–508 (2013).
23. Yuan, J.S. *et al.* Lunatic Fringe prolongs Delta/Notch-induced self-renewal of committed αβ T-cell progenitors. *Blood* **117**, 1184–1195 (2011).
24. Magri, M. *et al.* Notch ligands potentiate IL-7-driven proliferation and survival of human thymocyte precursors. *Eur. J. Immunol.* **39**, 1231–1240 (2009).
25. González-García, S. *et al.* CSL-MAML-dependent Notch1 signaling controls T lineage-specific IL-7Rα gene expression in early human thymopoiesis and leukemia. *J. Exp. Med.* **206**, 779–791 (2009).
26. Petrie, H.T., Hugo, P., Scollay, R. & Shortman, K. Lineage relationships and developmental kinetics of immature thymocytes: CD3, CD4, and CD8 acquisition in vivo and in vitro. *J. Exp. Med.* **172**, 1583–1588 (1990).
27. Ye, B.H. *et al.* The BCL-6 proto-oncogene controls germinal-centre formation and Th2-type inflammation. *Nat. Genet.* **16**, 161–170 (1997).
28. Dent, A.L., Shaffer, A.L., Yu, X., Allman, D. & Staudt, L.M. Control of inflammation, cytokine expression, and germinal center formation by BCL-6. *Science* **276**, 589–592 (1997).
29. Krangel, M.S. Mechanics of T cell receptor gene rearrangement. *Curr. Opin. Immunol.* **21**, 133–139 (2009).
30. Zhang, L., Reynolds, T.L., Shan, X. & Desiderio, S. Coupling of V(D)J recombination to the cell cycle suppresses genomic instability and lymphoid tumorigenesis. *Immunity* **34**, 163–174 (2011).
31. Maillard, I. *et al.* The requirement for Notch signaling at the β-selection checkpoint *in vivo* is absolute and independent of the pre-T cell receptor. *J. Exp. Med.* **203**, 2239–2245 (2006).
32. Nahar, R. *et al.* Pre-B cell receptor-mediated activation of BCL6 induces pre-B cell quiescence through transcriptional repression of MYC. *Blood* **118**, 4174–4178 (2011).
33. Inaba, H., Greaves, M. & Mullighan, C.G. Acute lymphoblastic leukaemia. *Lancet* **381**, 1943–1955 (2013).
34. Hagenbeek, T.J. *et al.* The loss of PTEN allows TCR alphabeta lineage thymocytes to bypass IL-7 and pre-TCR-mediated signaling. *J. Exp. Med.* **200**, 883–894 (2004).
35. Janas, M.L. *et al.* Thymic development beyond beta-selection requires phosphatidylinositol 3-kinase activation by CXCR4. *J. Exp. Med.* **207**, 247–261 (2010).
36. Pearce, L.R., Komander, D. & Alessi, D.R. The nuts and bolts of AGC protein kinases. *Nat. Rev. Mol. Cell Biol.* **11**, 9–22 (2010).
37. Hernandez-Munain, C., Roberts, J.L. & Krangel, M.S. Cooperation among multiple transcription factors is required for access to minimal T-cell receptor α-enhancer chromatin in vivo. *Mol. Cell. Biol.* **18**, 3223–3233 (1998).
38. Taghon, T., Yui, M.A., Pant, R., Diamond, R.A. & Rothenberg, E.V. Developmental and molecular characterization of emerging β- and γδ-selected pre-T cells in the adult mouse thymus. *Immunity* **24**, 53–64 (2006).
39. Amin, R.H. & Schlissel, M.S. Foxo1 directly regulates the transcription of recombination-activating genes during B cell development. *Nat. Immunol.* **9**, 613–622 (2008).
40. Johnson, K. *et al.* Regulation of immunoglobulin light-chain recombination by the transcription factor IRF-4 and the attenuation of interleukin-7 signaling. *Immunity* **28**, 335–345 (2008).
41. Timblin, G.A. & Schlissel, M.S. Ebf1 and c-Myb repress rag transcription downstream of Stat5 during early B cell development. *J. Immunol.* **191**, 4676–4687 (2013).

ONLINE METHODS

Mice. C57BL/6J (wild-type, *Il7r*$^{+/+}$*or Il7*$^{+/+}$) mice and *Il7r*$^{-/-}$ mice[42] mice were from Jackson Laboratories. *Il7*$^{-/-}$ mice[43] were provided by R. Gerstein. *BCL2*-transgenic mice crossed with *Il7r*$^{-/-}$ mice to generate *Il7r*$^{-/-}$*BCL2* mice have been described[44]. *Bcl6*$^{+/-}$ mice[27] were provided by R. Dalla-Favera. Genotypes were determined by PCR amplification of DNA obtained from tail tissue as described[44]. For all experiments, thymocytes were harvested from 4- to 6-week-old mice. All mice were bred in the specific pathogen–free facility of the Toronto Centre for Phenogenomics and procedures were approved by its Animal Care Committee, following guidelines from the Canadian Council on Animal Care.

Flow cytometry. Thymocyte single-cell suspensions were stained with fluorochrome-conjugated antibodies and secondary reagents, and immunofluorescence was analyzed on a FACSLSR-II (BD Biosciences) as described[23]. Data files were analyzed with FlowJo software (TreeStar). Dead cells and debris were excluded on the basis of staining with propidium iodide (unfixed cells) or Fixable Blue Viability dye (Invitrogen), versus forward-scatter profiles. Thymocytes were stained with a 'cocktail' of allophycocyanin-conjugated antibodies (all from BD Bioscience) specific for lineage markers (Lin) CD19 (1D3), Gr-1 (RB6-8C5), CD11b (M1/70), NK1.1 (PK136) and CD11c (HL3), together with fluorescein isothiocyanate–conjugated anti-CD71 (C2), and the following antibodies (all from e-Bioscience): Alexa Fluor 700–conjugated anti-CD3 (17A2), eFluor 450–conjugated anti-CD4 (RM4-5), allophycocyanin–eFluor 780–conjugated anti-CD8 (53-6.7), phycoerythrin-indotricarbocyanine–conjugated anti-CD25 (PC61.5), fluorescein isothiocyanate–conjugated anti-CD71 () and phycoerythrin-conjugated anti-CD98 (RL388). To distinguish DN2 from DN3 cells (**Fig. 2**), phycoerythrin-conjugated anti-CD44 (IM7; eBioscience) was used instead of anti-CD98. After Lin$^+$ cells were gated out, DN3a (CD25$^+$CD71^{lo}CD98^{lo}) thymocytes, DN3b (CD25$^+$CD71^{hi}CD98^{hi}) thymocytes and DN4 (CD25$^-$CD71^{hi}CD98^{hi} (*Il7*$^{+/+}$) or CD25$^-$CD71^{hi-lo}CD98^{hi-lo} (*Il7*$^{-/-}$)) thymocytes were sorted with a FACSAria II (BD Biosciences). Purity was >98% for all sorted populations. For detection of icTCRβ and mouse or human Bcl-2, cells were stained for 30 min at 4 °C with Fixable Blue Viability dye (Invitrogen), followed by antibodies specific for Lin markers together with antibodies specific for CD3, CD4, CD8a, CD25, CD71 and CD98 (identified above) before fixation, permeabilization (Cytofix/Cytoperm kit; BD Biosciences) and staining with anti-TCRβ (H57-597), anti–mouse Bcl-2 (3F11) or anti–human Bcl-2 (6C8) according to the manufacturer's protocols (BD Biosciences).

The following fluorochrome- or biotin-conjugated antibodies specific for mouse markers were used where needed: anti-IL-7R (A7R34), anti-CD45.1 (A20), anti-CD45.2 (104), anti-CD25 (7D4), anti-Ly76 (Ter119), anti-CD24 (M1/69), anti-CD27 (LG.3A10) and anti-CD117 (2B8). Antibody-fluorochrome conjugates and Avidin second-stage reagents were from Pharmingen–BD Biosciences or eBioscience and were used at predetermined optimal concentrations. Statistical significance for all population comparisons was calculated with unpaired two-tailed *t*-tests. Fluorescence-minus-one controls included all antibodies except the one on the horizontal axis in each figure.

For analysis of thymocyte proliferation *in vivo*, 4- to 6-week-old *Il7r*$^{-/-}$ and *Il7r*$^{-/-}$*BCL2* mice and age-matched *Il7r*$^{+/+}$ mice were injected twice with 1 mg BrdU (intraperitoneally), 1 h apart. Thymocytes were isolated 2, 24 or 48 h after the first injection. BrdU incorporation was assessed after Fixable Blue staining with a BrdU Flow Kit according to the manufacturer's instructions (BD Biosciences).

Staining of phosphorylated STAT5. For *ex vivo* experiments, thymocyte suspensions were prepared in serum-free, phenol-free RPMI medium (Wisent), then were stained for 30 min at 37 °C with Fixable Blue and were immediately fixed with BD Cytofix buffer and then permeabilized with Phosphoflow BD Perm III buffer before being stained with Alexa Fluor 647–conjugated antibody to STAT5 phosphorylated at Tyr694 (47; BD Biosciences) and anti-TCRβ, anti-CD4, anti-CD8, anti-CD25 and anti-CD27 (all identified above). For detection of phosphorylated STAT5 after *in vitro* stimulation with IL-7, wild-type thymocytes were cultured for 20 min with medium alone or 10 ng/ml mouse IL-7, were then stained for 30 min at 37 °C with Fixable Blue and fixed and permeablized as described above before being stained with the appropriate antibodies (identified above).

Cell culture. Sorted thymocytes were seeded into 24-well plates containing 1 ml Iscove's media supplemented with 20% FBS, penicillin (100 U/ml), streptomycin (100 μg/ml) and IL7 (10 ng/ml), and were incubated at 37 °C in a humidified atmosphere with 5% CO_2 for the amount of time indicated in the relevant figure legend. For analysis of thymocyte proliferation *in vitro*, wild-type DN4 thymocytes were sorted and labeled with CFSE (carboxyfluorescein diacetate succinimidyl ester)) as described[23] before culture (5×10^3 cells per well) in medium alone or with 10 ng/ml of IL7 without stromal cells, or on 80%-confluent monolayers of OP9-DL4 cells together with increasing doses of IL-7 (0, 0.05, 0.5 and 5 ng/ml). After 15-40 h (no stroma) or 48 h (on OP9-DL4 cells), cells were stained with propidium iodide, followed by anti-CD4 and anti-CD8 (both identified above), and CFSE levels and viable cell numbers were assessed by flow cytometry.

For analysis of the effect of *Bcl6* deletion on the survival of DN4 cells *in vitro,* Ter119$^-$CD19$^-$Gr-1$^-$CD117$^+$ cells from *Bcl6*$^{-/-}$ and *Bcl6*$^{+/+}$ fetal liver (15.5 d after coitus) were sorted and cultured (1×10^3 cells per well) together with OP9-DL4 cells and with IL-7 and the cytokine Flt3L as described[23], to induce their differentiation into precursors of the T cell lineage. After 9 d, DN4 cells (Lin$^-$CD45.2$^+$CD4$^-$CD8$^-$CD44$^-$CD25$^-$CD27^{hi}) were sorted and re-cultured (3×10^3 cells per well) on OP9-DL4 cells in medium alone or with IL-7 (10 ng/ml). After 2 d, expression of CD4 and CD8 and recovery of viable icTCRβ$^+$ DN cells were quantified by flow cytometry.

Gene-expression profiling. DN3a, DN3b and DN4 thymocytes were sorted from *Il7r*$^{+/+}$ mice (four independent sorts), were allowed to 'rest' for 1 h at 37 °C in a humidified atmosphere with 5% CO_2, and then were left untreated or were stimulated for 3 h with IL-7 (10 ng/ml; Stem Cell Technologies) before isolation of total cellular RNA with an RNeasy isolation kit (Qiagen). A Bioanalyzer 2100 (Agilent) was used for quality control and quantification. Illumina MouseRef-8 v2.0 Expression BeadChip kits were used for genome-wide expression profiling according to standard protocols at The Centre for Applied Genomics core facility at the Hospital for Sick Children. R Bioconductor 2.13.0 software was used for data processing and other statistical analyses. Raw signals from 25,697 probes were pre-processed for background subtraction, quantile normalization and $\log_2$ transformation before the use of moderated *t*-tests from the Bioconductor software package Limma (linear models for microarray data). Empirical Bayes smoothing was applied to the standard errors. Paired *t*-tests were used for the identification of IL-7-induced changes in gene expression in each subset, and the false-discovery rate (FDR) was estimated with the Benjamini-Hochberg method to correct for multiple testing. Pearson correlations showed that technical replicates had very high correlations between chips. For genes represented by multiple probe sets on the array, we selected the ones with the highest ANOVA F-statistics (lowest FDR-adjusted *q* value).

Gene set–enrichment analysis. Gene lists were ranked using the Limma moderated *t*-statistic, a value that reflects the magnitude of differences in expression (based on mean expression value) as well as the variance of that gene's expression within each group. Parameters were set to 2,000 gene-set permutations and gene-set sizes between 15 and 500. Gene sets were obtained from the following databases: KEGG, MsigDB-c2, NCI, Biocarta, IOB, Netpath, HumanCyc, Reactome and Gene Ontology. Enrichment maps showing relationships between gene sets with significant enrichment (nominal *P* value, <0.01; overlap coefficient, 0.5) were generated with the Enrichment Plugin module (v1.2) of the Cytoscape 2.8.1 software platform[45].

Quantitative RT-PCR. mRNA from sorted thymocytes was isolated with an RNeasy Plus Micro kit (Qiagen) and was reverse-transcribed with a High Capacity cDNA Reverse Transcription Kit (Life Technologies). The abundance of *Cd45*, *Bcl6, Rag1* and *Rag2* cDNA in each sample was determined with Power SYBR Green (Life Technologies). The primers used were as follows: *Cd45* forward, 5′-AAGTCTCTACGCAAAGCACGG-3′, *Cd45* reverse, 5′-GATAGATGCTGGCGATGATGTC-3′, *Bcl6* forward,

doi:10.1038/ni.3122

5′-CTGCAGATGGAGCATGTTGT-3′, *Bcl6* reverse, 5′-GCCATTTCTGCT TCACTGG-3′, *Rag1* forward, 5′-CTGTGGCATCGAGTGTTAACA-3′, *Rag1* reverse, 5′-GCTCAGGGTAGACGGCAAG-3′, *Rag2* forward, 5′-TG CCAAAATAAGAAAGAGTATTTCAC-3′, *Rag2* reverse, 5′-GGGACATTT TTGATTGTGAATAGG-3′. The number of *Bcl6, Rag1* and *Rag2* templates was divided by the number of *Cd45* templates (mean of triplicate measurements) to obtain normalized expression values for each gene.

***Tcra* recombination.** Genomic DNA was isolated from sorted thymocytes by standard procedures. Rearranged DNA was quantified by real-time PCR with a QuantiFast SYBR Green PCR kit (Qiagen). All PCR reactions were run in duplicate with the following amplification program: 95 °C for 5 min, followed by 45 cycles of 95 °C for 10s and 62 °C for 30s. Samples were normalized to signals for the gene encoding β_2-microglobulin (*B2m*). Primers used for analysis of *Tcra* rearrangements have been published[46–48], except for *Tcra-J30* (GGGAGAACATGAAGATGTGTCC).

Immunoblot analysis. Protein extracts were prepared from sorted thymocytes in modified radioimmunoprecipitation assay (RIPA) buffer (50 mM tris-Cl (pH 7.4), 1% NP-40, 0.25% sodium deoxycholate, 150 mM NaCl and 1 mM EDTA) with protease inhibitor (Roche) and were separated by SDS-PAGE. Proteins were transferred onto polyvinylidene difluoride membranes, which were cut into two parts at the level of the 50-kilodalton marker before immunoblot analysis overnight by standard techniques. The upper membrane was probed with rabbit anti-RAG-2 (EPRAGR239; Abcam), and the lower membrane was probed with rabbit anti-β-actin (13E5; Cell Signaling). Both membranes were then probed for 2 h with horseradish peroxidase–conjugated antibody to rabbit immunoglobulin G (7074; Cell Signaling). Proteins were detected with ECL reagents (GE Healthcare) and were digitally measured with ChemiDoc MP (Bio-Rad).

Statistical methods. Data were analyzed with a two-tailed Student *t*-test for comparison of the means of two groups and by one-way ANOVA with Newman-Keuls post-hoc *t*-test for comparison of the means of two groups in experiments with three or more groups. *P* values of less than 0.05 were considered statistically significant. No randomization of mice or 'blinding' of researchers to sample identity was used during the analyses. Sample sizes were not predetermined on the basis of expected effect size, but rough estimations were made on the basis of pilot experiments and measurements. No data exclusion was applied.

42. Peschon, J.J. *et al.* Early lymphocyte expansion is severely impaired in interleukin 7 receptor-deficient mice. *J. Exp. Med.* **180**, 1955–1960 (1994).
43. von Freeden-Jeffry, U. *et al.* Lymphopenia in interleukin (IL)-7 gene-deleted mice identifies IL-7 as a nonredundant cytokine. *J. Exp. Med.* **181**, 1519–1526 (1995).
44. Matei, I.R. *et al.* ATM deficiency disrupts Tcra locus integrity and the maturation of $CD4^+CD8^+$ thymocytes. *Blood* **109**, 1887–1896 (2007).
45. Smoot, M.E., Ono, K., Ruscheinski, J., Wang, P.L. & Ideker, T. Cytoscape 2.8: new features for data integration and network visualization. *Bioinformatics* **27**, 431–432 (2011).
46. Abarrategui, I. & Krangel, M.S. Regulation of T cell receptor-α gene recombination by transcription. *Nat. Immunol.* **7**, 1109–1115 (2006).
47. Shih, H.Y. *et al. Tcra* gene recombination is supported by a *Tcra* enhancer- and CTCF-dependent chromatin hub. *Proc. Natl. Acad. Sci. USA* **109**, E3493–E3502 (2012).
48. Vacchio, M.S., Olaru, A., Livak, F. & Hodes, R.J. ATM deficiency impairs thymocyte maturation because of defective resolution of T cell receptor α locus coding end breaks. *Proc. Natl. Acad. Sci. USA* **104**, 6323–6328 (2007).